Iranian Journal of Science and Technology, Transactions of Civil Engineering (2020) 44:787–802
https://doi.org/10.1007/s40996-019-00296-6

RESEARCH PAPER

Optimum Design of Tuned Mass Dampers Using Colliding Bodies Optimization in Frequency Domain

Maziar Fahimi Farzam[1] · Ali Kaveh[2]

Received: 10 February 2019 / Accepted: 22 July 2019 / Published online: 26 July 2019

Abstract
Optimum design parameters of tuned mass dampers are calculated as a function of damper to structure mass ratio and inherent damping ratio of the main structure in frequency domain. A robust control algorithm is adopted in order to assure response reduction in controlled structure subjected to different earthquakes, and an equivalent single degree-of-freedom structure is introduced to reduce the computation cost of optimum design. H_∞ norm minimization of this equivalent structure is considered as the objective function. Considering inherent structural damping for main structure, the recently developed metaheuristic algorithm known as CBO is used to find the optimum values of the design parameters. Using the proposed procedure, design charts are prepared for a 10-story shear building.

Keywords Tuned mass dampers · Earthquake excitation · Metaheuristic algorithm · H_∞ norm · Robust control

1 Introduction

In recent decades, control systems have been widely utilized to reduce the response of tall and super-tall buildings subjected to lateral loads. Passive control devices are one of the great categories of these systems commonly studied in past centuries. TMDs are the most established devices in this category used in many constructed buildings all over the world because of its simple, reliable and economical system. A comprehensive list of structures using TMD as their control device can be found in the work of Gutierrez Soto and Adeli (2013). The 60-story John Hancock in Boston having two 300-ton TMDs is one of the first controlled buildings with TMD that has been constructed in 1977 to reduce the building response under wind vibrations. One of the famous examples includes the 101-story Taipei 101 in Taipei having a 730-ton TMD and constructed in 2004 (Gutierrez Soto and Adeli 2013). The 125-story Shanghai Center Tower in Shanghai is the second tallest building in the world being opened since 2017. It is a super-tall landmark which has the heaviest TMD (about 1000-ton) ever designed (Lu et al. 2016).

The main concept of TMD is very simple, and probably it was first introduced by Frahm in 1909. Figure 1a shows the TMD primary concept, composed of a main mass and its stiffness, represented by M and K, whereas the mass and stiffness of the damper are denoted with m_d and k_d, respectively. In the literature, this configuration has been tested under the main mass harmonic excitation, and it has been ascertained that if the damper frequency is set equal to the excitation frequency, the main mass displacement response will be zero. If the excitation frequency gets close to the structural natural frequency, the structural response could increase significantly, so in broadband excitation, the TMD frequency is set equal to the structural natural frequency to prevent resonance.

The proposed setup of Fig. 1a is effective only if the excitation frequency is equivalent to the damper frequency, and its favorable performance decreases significantly by changing the excitation frequency content. Therefore, in order to overcome this drawback, Den Hartog added a viscous damper to the auxiliary mass (Fig. 1b). Additionally, to get a better performance from the damper, its characteristics should be adjusted such that the main structural response is minimum. In the preliminary investigations, the vibration equations were solved in frequency domain. Den Hartog developed the fixed point method to calculate

✉ Ali Kaveh
alikaveh@iust.ac.ir

1 Department of Structural Engineering, University of Maragheh, Maragheh, Iran

2 School of Civil Engineering, Iran University of Science and Technology, Narmak, Tehran 16846-13114, Iran

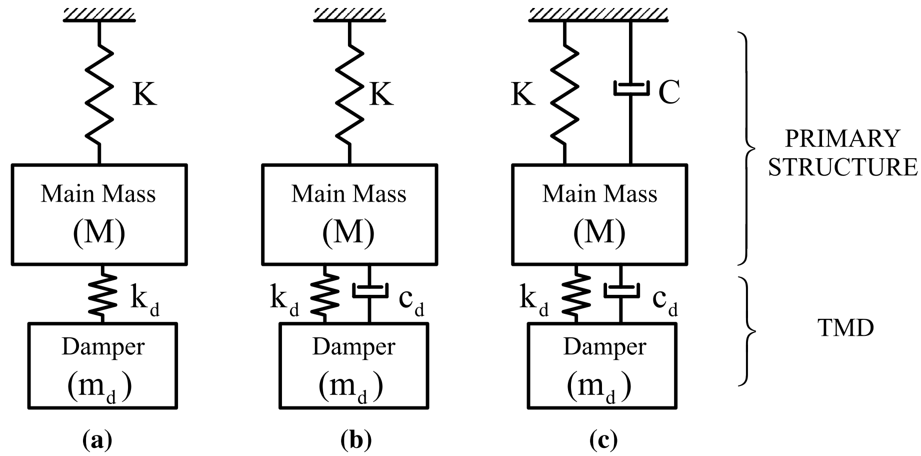

Fig. 1 Development of TMD concept: **a** Frahm model (Den Hartog 1947), **b** Den Hartog model (Den Hartog 1947), **c** Warburton Model (Warburton 1982)

the optimum free parameters of tuned mass dampers. This tuning approach utilizes the feature that the controlled system transfer function passes through two fixed points for any damping ratio after mounting TMD. As a result, the free parameter optimum values are evaluated in a two-step procedure. In the first step, the frequency ratio is selected to equalize the peak amplitude of these two fixed points, and in the next step, two damping ratios are determined in a manner that for each of them the transfer function passes horizontally through the invariant points. Eventually, the mean of these two damping ratios is considered as the optimum value of the TMD damping.

Furthermore, Den Hartog proposed closed-form expressions for optimum design parameters (frequency and damping ratio) based on the fixed point approach. Den Hartog formulae are derived for mass excitation without considering inherent structural damping; thus, other researchers, e.g., Ioi and Ikeda (1978) and Warburton (1982) have developed different formulae by considering inherent structural damping under base excitation (Fig. 1c).

At the end of the past century, researchers started to assess the performance of TMDs on multi-degree-of-freedom (MDOF) structures under earthquake excitations. Figure 2 illustrates an *N*-story shear building with a TMD added on its roof. In this category, the distinguished work of Villaverde (1985), Sadek et al. (1997), Gutierrez Soto and Adeli (2014) and Salvi and Rizzi (2016) on the performance of TMDs attached on shear buildings can be mentioned. In Table 1, a brief of closed-form formulae represented in the literature are reviewed.

The proposed expressions in Table 1 show the optimum TMD parameters dependency on damper to structure mass ratio, the ratio of structural damping to its critical damping, and the amplitude of mode shape in control mode at the location of TMD denoted as μ, ξ_s and φ, respectively. It should be noted that the last two variables (μ and φ) are calculated for a unit modal participation factor.

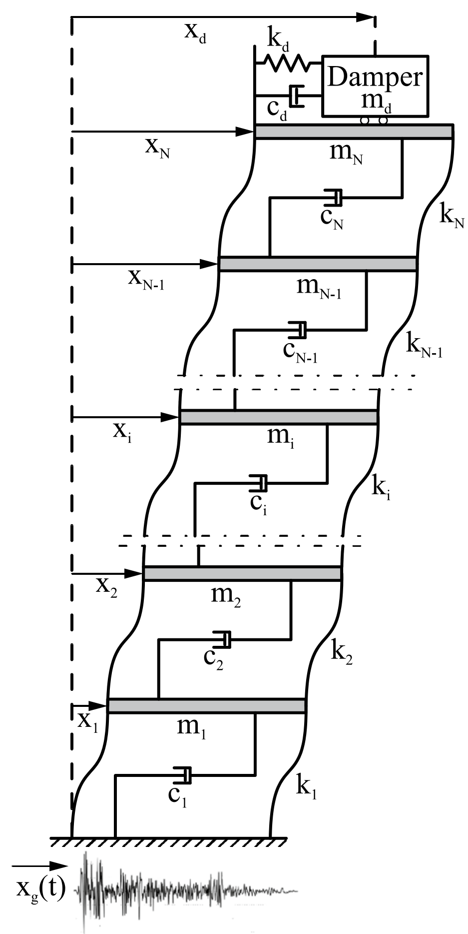

Fig. 2 An N degree-of-freedom structure with a TMD under earthquake excitation

In one of the last studies conducted in TMD context, Salvi and Rizzi (2016) utilized a gradient method and computed optimum TMD parameters under different harmonic and white noise base or structural mass excitations. They derived new and simple closed-form equations to determine tuning parameters used for comparison in our study.

Table 1 Closed-form expressions for tuning free parameters of TMD

Methods	Year	$f_{\text{opt}} = \frac{\omega_{\text{d,opt}}}{\omega_{\text{s}}}$	$\xi_{\text{d,opt}} = \frac{c_{\text{d,opt}}}{2m_{\text{d}}\omega_{\text{d,opt}}}$
Frahm (Den Hartog 1947)	1909	1	–
Den Hartog (Den Hartog 1947)	1956	$\frac{1}{1+\mu}$	$\sqrt{\frac{3\mu}{8(1+\mu)}}$
Villaverde (Villaverde 1985)	1985	1	$\xi_{\text{s}} + \phi\sqrt{\mu}$
Sadek et al. (Sadek et al. 1997)	1997	$\frac{1}{1+\phi\mu}\left[1 - \xi_{\text{s}}\sqrt{\frac{\phi\mu}{1+\phi\mu}}\right]$	$\phi\left(\frac{\xi_{\text{s}}}{1+\mu} + \sqrt{\frac{\mu}{1+\mu}}\right)$
Salvi & Rizzi (Salvi and Rizzi 2016)	2016	$1 - \sqrt{3\mu}\left(\frac{2}{3}\sqrt{\mu} + \frac{3}{2}\zeta_{\text{s}}\right)$	$\frac{1}{2}\sqrt{\mu}$

Although the mass ratio (μ) has been used as tuning parameters in some studies, in others, its value is preselected because of the construction limitation. Thus, concerning this limitation, TMD mass is generally selected between 1 and 15% of the main mass. Additionally, the value of inherent structural damping ratio could be selected 20% maximum. However, in many buildings and other structures, damping ratio is under 10%, so the upper bound of inherent structural damping ratio is considered as 10%.

MDOF structures can take advantage of TMD to control a specific vibration mode; however, in these structures, multi-tuned mass damper (MTMD) that is not dealt with in this study can be utilized to control multi-modes.

New definitions for f and μ are necessary for MDOF structures. Common definitions presented in the previous analyses were based on the controlled-mode effective mass and frequency, so to control a shear building, if just a TMD is used, it is better to control the first mode. In shear buildings, the first mode has the most contribution in the structural response, so the frequency and mass ratios of the MDOF are chosen the same as a SDOF but just for the frequency and the effective mass of the first vibration mode (Sadek et al. 1997).

Tuning a TMD for MDOF structures is more complicated in comparison with SDOF structures, so during the two recent decades, many different metaheuristic algorithms have been implemented to find out the TMD optimum parameters for MDOF structures and until today, every year many different researches are being conducted in this field. Probably, the first use of metaheuristic algorithm on TMD context is the work of Hadi and Arfiadi (1998) which found the TMD optimum parameters with genetic algorithm. Furthermore, other metaheuristics such as real-coded genetic algorithm, ant colony, bee colony, particle swarm optimization, harmony search, charged system search, flower pollination have been implemented to estimate the optimum TMD parameters (Arfiadi 2016; Bekdas and Nigdeli 2011; Farshidianfar and Soheili 2013a, b, c; Nigdeli et al. 2016; Bekdas and Nigdeli 2017a, b; Leung et al. 2008; Leung and Zhang 2009; Kaveh et al. 2015). In this study, the colliding bodies optimization (CBO) algorithm (Kaveh and Mahdavi (2014); Kaveh (2017a, b)), as one of the most recent metaheuristic algorithms, is utilized to determine the optimum TMD parameters. The main feature of CBO is its parameter independence. However, in this paper any other metaheuristics can be used, see for example, Kaveh (2017a, b). The derived results are then compared with those of the closed-form formulae from the literature.

The rest of this paper is structured as follows. The second section briefly introduces the CBO and its pseudocode as applied in the present study. Dynamic notation and formulation for shear building in time and frequency domain are reviewed in the third section. In the fourth section, the optimization steps are presented. In the fifth section, the optimum values of the TMD tuning parameters are calculated and compared with those of the previous researches, and in the sixth section, the controlled structure performance is evaluated and compared to the closed-form expressions presented in the literature. Finally, in the last section, the concluding remarks are outlined.

2 Colliding Bodies Optimization Algorithm

Having simple formulation, the CBO is one of the metaheuristic algorithms recently proposed by Kaveh and Mahdavi (2014), and it needs no internal parameter tuning. Additionally, it belongs to the population-based metaheuristics which takes inspiration from physical laws of rigid body collisions. This method makes a population of solutions in each step with each of them being represented with a colliding body (CB). With ordering the solutions based on their fitness values, a mass is assigned to each CB proportioned inversely to its fitness value. In minimization problems, the mass of each CB is calculated based on the following formula:

$$\text{mass}_i = \frac{\frac{1}{\text{fit}(\text{CB}_i)}}{\sum_{j=1}^{2N} \frac{1}{\text{fit}(\text{CB}_j)}} \tag{1}$$

where mass_i denotes the attributed mass of body i, $2N$ is the number of CBs, and $\text{fit}(\text{CB}_\text{i})$ is the value of objective function for the agent i. Based on the above equation, the mass of a CB will increase by decreasing its fitness value. These properties are illustrated schematically in Fig. 3. Then, all arranged CBs are divided into two parts with equal number of members. The first part whose fitness function has better quality is considered as stationary, and each CB in the second part moves toward its corresponding bodies in the first part with velocity proportioned to the difference in their fitness values. Based on governing physical laws of colliding bodies, CB velocities after collision are specified as a function of masses and the CB velocities before collision. Consequently, the position of CBs is determined based on their new velocity, and this procedure is continued until the specified termination condition is fulfilled.

The CBO pseudocode for a minimization problem is as follows (Kaveh and Mahdavi 2014):

Set initial position for 2N-CBs randomly
Repeat
For each CB, the objective function is calculated
The mass of CBs is assigned inversely proportioned to its fitness value
The CBs are lined up in ascending order based on their mass
The organized CBs are divided into two parts
The CBs in the second part move toward their relevant CBs in the first part.
CBs are colliding with each other, and their velocity after collision is evaluated
The new positions of CBs are calculated based on their after collision velocities
Until the termination criteria is fulfilled.
Output: founded best solution

In this study, the number of CBs and steps that are used in the optimization process is 20 and 30, respectively.

3 Mathematical Models for Structural Vibration

In this section, three different mathematical models used for structural vibration assessment are briefly introduced. These three models are differential equation, state space representation (system of first-order differential equations) and transfer function (output to input Laplace ratio). The first model is used for modal analysis and the numerical example seismic performance assessment. The second model is employed for simple representation of vibration equation and calculation of the transfer function. Finally, the H_∞ norm of equivalent structure transfer function of the shear building first mode is considered as the objective function in the optimization algorithm.

3.1 Differential Equation

The vibration equation of a MDOF structure subjected to an external excitation is represented by Eq. (2) (Chopra 2001):

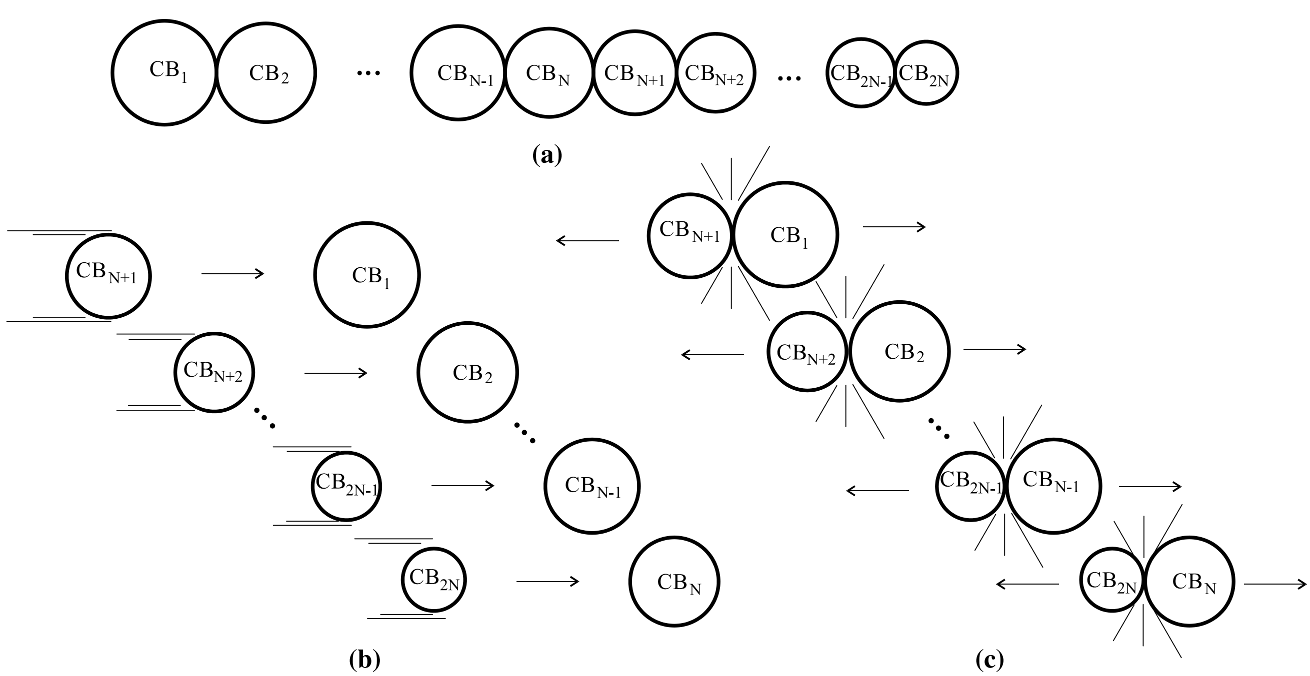

Fig. 3 CBO algorithm steps: **a** CBs sorted in increasing order **b** before the collision **c** after the collision

$$\boldsymbol{M}\ddot{\boldsymbol{X}}(t) + \boldsymbol{C}\dot{\boldsymbol{X}}(t) + \boldsymbol{K}\boldsymbol{X}(t) = \boldsymbol{U}(t) \tag{2}$$

where for a structure with N degree-of-freedom, $\boldsymbol{M}$, $\boldsymbol{C}$ and $\boldsymbol{K}$ are mass, damping and stiffness matrices, respectively, having dimension $N \times N$. In addition, $\boldsymbol{X}(t)$, $\dot{\boldsymbol{X}}(t)$ and $\ddot{\boldsymbol{X}}(t)$ are structural displacement, velocity and acceleration vectors with respect to the ground, and $\boldsymbol{U}(t)$ is the external force vector, all of which have the dimension $N \times 1$. In Fig. 2, the N degree-of-freedom structure with a TMD is shown.

If a TMD is added to the roof of the structure, one degree-of-freedom will be added to the system, and the matrices $\boldsymbol{M}$, $\boldsymbol{C}$, $\boldsymbol{K}$ and the vector $\boldsymbol{X}(t)$ for $(N+1)$ degree-of-freedom system will be defined as Eqs. (3)–(6):

$$\boldsymbol{M} = \mathrm{diag}[m_1 \quad m_2 \ldots \quad m_N \quad m_d] \tag{3}$$

$$\boldsymbol{K} = \begin{pmatrix} k_1 + k_2 & -k_2 & & & & \\ -k_2 & k_2 + k_3 & -k_3 & & & \\ & & & \ddots & & \\ & & & -k_N & k_N + k_d & -k_d \\ & & & & -k_d & k_d \end{pmatrix} \tag{4}$$

$$\boldsymbol{C} = \begin{pmatrix} c_1 + c_2 & -c_2 & & & & \\ -c_2 & c_2 + c_3 & -c_3 & & & \\ & & & \ddots & & \\ & & & -c_N & c_N + k_d & -c_d \\ & & & & -c_d & c_d \end{pmatrix} \tag{5}$$

$$\boldsymbol{X}(t) = [x_1 \quad x_2 \ldots \quad x_N \quad x_d]^{\mathrm{T}} \tag{6}$$

where the (i) and (d) indices are used to show the ith floor parameters and damper parameters, respectively, as shown in Fig. 2. Response history analysis of a structure under earthquake excitation is a step-by-step procedure which calculates the dynamic response of the structure in time domain during and after the earthquake. This analysis is performed in MATLAB software with direct integral method.

3.2 State Space

Writing the equation of motion in state space makes dynamic system modeling and analyzing simpler, so in this research, the state space form of vibration equation is addressed. In the state space, the second-order differential equation of motion is reduced to a system of first-order differential equations, which have a closed-form solution, so the vibration equations in state space are (Soong 1990; Debnath et al. 2013):

$$\dot{\boldsymbol{Z}}(t) = \boldsymbol{A}\boldsymbol{Z}(t) + \boldsymbol{B}\boldsymbol{U}(t) \tag{7}$$

$$\boldsymbol{X}(t) = \boldsymbol{C}\boldsymbol{Z}(t) \tag{8}$$

In this equation, if the system has N degree-of-freedom, $\boldsymbol{Z}(t)$ is a $2N \times 1$ vector, $\boldsymbol{A}$ is a system matrix by dimension $2N \times 2N$, $\boldsymbol{B}$ is a location matrix with dimension $2N \times 1$, and $\boldsymbol{C}$ is a matrix dependent on the desired output. The matrices $\boldsymbol{A}$ and $\boldsymbol{B}$ and the vector $\boldsymbol{Z}(t)$ are defined in the following equations:

$$\boldsymbol{A} = \begin{bmatrix} \boldsymbol{0} & \boldsymbol{I} \\ -\boldsymbol{M}^{-1}\boldsymbol{K} & -\boldsymbol{M}^{-1}\boldsymbol{C} \end{bmatrix} \tag{9}$$

$$\boldsymbol{B} = \begin{bmatrix} \boldsymbol{0} \\ \boldsymbol{I} \end{bmatrix} \tag{10}$$

$$\boldsymbol{Z}(t) = [x_1 x_2 \ldots x_N \dot{x}_1 \dot{x}_2 \ldots \dot{x}_N]^{\mathrm{T}} \tag{11}$$

where $\mathbf{0}$ and $\mathbf{I}$ are zero and identity matrices, respectively.

3.3 Transfer Function

Transfer function is calculated by Fourier and Laplace transform of Eqs. (7) and (8). In this case, by means of Fourier transformation the transfer function is:

$$\boldsymbol{H}(\omega) = \boldsymbol{C}(i\omega\boldsymbol{I} - \boldsymbol{A})^{-1}\boldsymbol{B} \tag{12}$$

In this equation, $i = \sqrt{-1}$ and using transfer function concept, the vibration equation is represented as:

$$\boldsymbol{X}(\omega) = \boldsymbol{H}(\omega)\boldsymbol{U}(\omega) \tag{13}$$

The H_∞ norm considered as the objective function in this study is defined as follows:

$$\|\boldsymbol{H}(\omega)\|_\infty = \sup_{\omega} \ \bar{\sigma}(\boldsymbol{H}(\omega)) \tag{14}$$

In this equation, $\bar{\sigma}$ means the greatest singular value of the transfer function matrix and $\sup_\omega$ means the smallest higher bound of this relation over all frequencies.

4 Optimization Procedure

Generally, two main schools of thoughts have been pursued in the previous investigations for optimum design of TMDs (Salvi and Rizzi 2011). In the first school of thought, independent of external loading frequency content, the optimum parameters are obtained, e.g., in frequency domain, under the white noise excitation (Den Hartog 1947; Asami et al. 2002; Warburton 1982; Salvi and Rizzi 2017; Leung et al. 2008; Leung and Zhang 2009, etc.) or by other methods such as Villaverde (1985) or Sadek et al. (1997). In the second school of thought, TMD optimum parameters are calculated under a deterministic earthquake or harmonic excitation (Bekdas and Nigdeli 2011; Farshidianfar and Soheili 2013a, b, c; Nigdeli et al. 2016; Bekdas and Nigdeli 2017a, b; Kaveh et al. 2015), i.e., the performance of the derived results is dependent on the excitation frequency content; however, in some of these researches, techniques have been used to solve this problem. In this paper, efforts have been made for it to be based on the first school of thought with a simple procedure and somehow different from previous researches, optimization is simply and quickly performed, and then design graphs are generated for optimum design of TMD. Therefore, the transfer function infinity norm is preferred as the objective function. Thus, the optimum parameters are independent from external excitations frequency content, and the control method is robust. However, to make the optimization more efficient and to consider the importance of the first mode in final response, an equivalent SDOF structure is defined based on the first mode characteristics, and the TMD optimum parameters are obtained for this equivalent structure.

For the SDOF system, if the damper frequency (ω_d) and structural frequency (ω_s) are defined as Eq. (15), the frequency and damping ratios defined by Eq. (16) are considered as TMD free parameters, and the optimum values of these parameters are determined such that the structural response is minimized.

$$\omega_d = \sqrt{\frac{k_d}{m_d}}, \quad \omega_s = \sqrt{\frac{K}{M}} \tag{15}$$

$$f = \frac{\omega_d}{\omega_s}, \quad \xi_d = \frac{c_d}{2m_d\omega_d} \tag{16}$$

In Eq. (16), the frequency ratio (f) is defined as the auxiliary mass frequency to main mass frequency, and the damping ratio (ξ_d) is defined for the damper with the ratio of its damping to the critical damping. In the latter equation, c_d and m_d are the damping and the mass of damper, respectively.

General steps of the TMD optimum parameters calculation for this equivalent structure are as follows:

1. A frequency analysis is performed, and natural frequencies and modal shapes are realized.
2. Dynamical properties of the first mode (mass, stiffness and damping) are determined, and an equivalent SDOF structure is constructed.
3. CBO algorithm is employed to find the TMD optimum parameters as a function of mass ratio and different inherent structural damping ratios. In this procedure, transfer function H_∞ norm of the equivalent structure is selected as the objective function, and the frequency and damping ratios are applied as the design variables. In MATLAB vector notation, the range of tuning values is considered as follows:

$$f = [0:0.005:0.5], \quad \xi_d = [0.55:0.01:1.2] \tag{17}$$

4. TMD optimum free parameters as a function of mass ratio (μ) and inherent structural damping ratio ξ_s are computed. Results are presented in design graphs in which optimum parameters are calculated based on the proposed method and compared with the closed-form formulae presented in the literature.

5 Numerical Example

In this section, a benchmark shear building is assessed (Salvi and Rizzi 2011; Sadek et al. 1997) which is depicted in Fig. 4a as a planar linear 10-story frame structure. This structure is modeled as a 10-DOF dynamic system with mass m_k ($k=1, 2, \ldots, 10$) lumped at the k-th floor. The structural properties are represented in Table 2, and an equivalent SDOF structure is shown in Fig. 4b. In this building, a TMD on the top of the structure is added to control the structural responses under external excitations.

Optimum free parameters at different values of mass ratio (μ) and four different inherent structural damping ratios ($\xi_s = 0$, 2, 5 and 10%) are calculated, and optimum

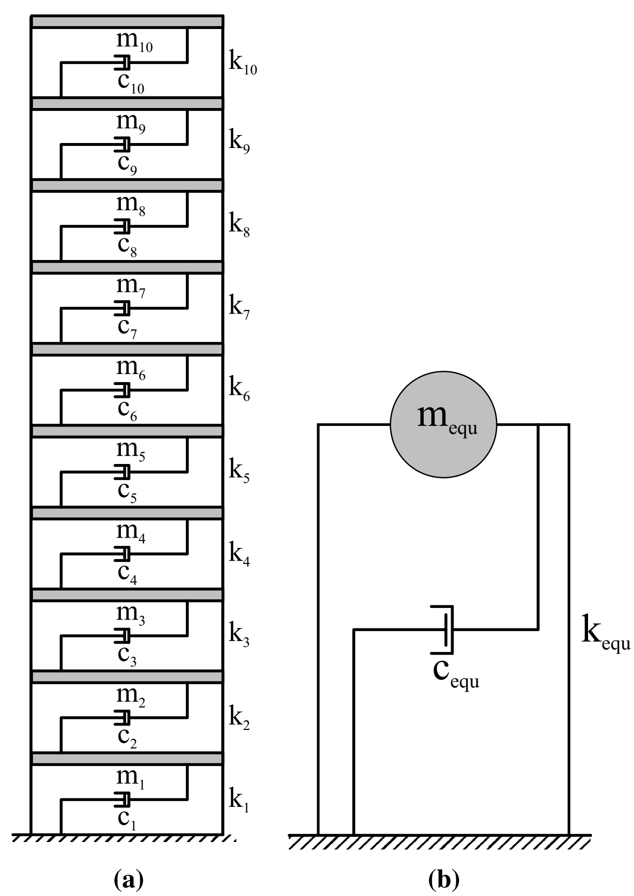

Fig. 4 Design example structure: **a** the 10-story shear building, **b** the equivalent SDOF structure

Table 2 Structural parameters of the 10-story building (Salvi and Rizzi 2011)

Story	Mass ($\times 10^3$ kg)	Stiffness ($\times 10^6$ N/m)	Circular frequency (rad/s)	Period (s)	Story	Mass ($\times 10^3$ kg)	Stiffness ($\times 10^6$ N/m)	Circular frequency (rad/s)	Period (s)
1	179	62.47	0.50037	0.99853	6	134	46.79	4.29197	0.23299
2	170	59.26	1.32631	0.75397	7	125	43.67	4.83577	0.20680
3	161	56.14	2.15121	0.46485	8	116	40.55	5.27169	0.18969
4	152	53.02	2.93387	0.34085	9	107	37.43	5.59050	0.17887
5	143	49.91	3.65320	0.27373	10	98	34.31	5.78653	0.17282

values of the free parameters are plotted as a function of μ in Figs. 5 and 6. In these figures, closed-form formulae from Villaverde (1985), Sadek et al. (1997) and Salvi and Rizzi (2017) derived for MDOF structures are plotted for comparison. As can be seen, the present tuning procedure has the same general pattern with respect to those proposed in the literature; however, the obtained trend of optimum frequency and damping ratios have the most similarity to Sadek et al. (1997) and Salvi and Rizzi (2017) estimation, respectively. It should be noted that Sadek et al. (1997) revealed the detuning effect of Villaverde (1985) formula when the mass ratio is increased. They displayed that if the frequency ratio is set equal to one, by increasing the mass ratio, optimum parameters determined based on Villaverde (1985) method are not optimum.

To assure the acceptable performance of CBO, the H_∞ norm ratio of controlled to uncontrolled structure at different values of damping and mass ratios near the optimum values are calculated and illustrated in Fig. 7 at $\mu = 0.05$ and each of four different inherent structural damping ratios. The convergence histories of the CBO algorithm are displayed in Fig. 8 for these four cases.

Figure 7 illustrates the search landscape and the position of optimum points in the search space. Additionally, it can be seen that by reducing the damping ratio in the main structure, the TMD effect is increased considerably, and the sensitivity of the system to the change of free parameters is reduced. Another point, which should be noted, is the shape of regions with equal transfer function amplitude which is almost a horizontal ellipse, so the response sensitivity to the damping change is smaller than the frequency change.

In this example, although the convergence speed of the optimization process is appropriate, if a larger structure with more constraints wants to be optimized, some

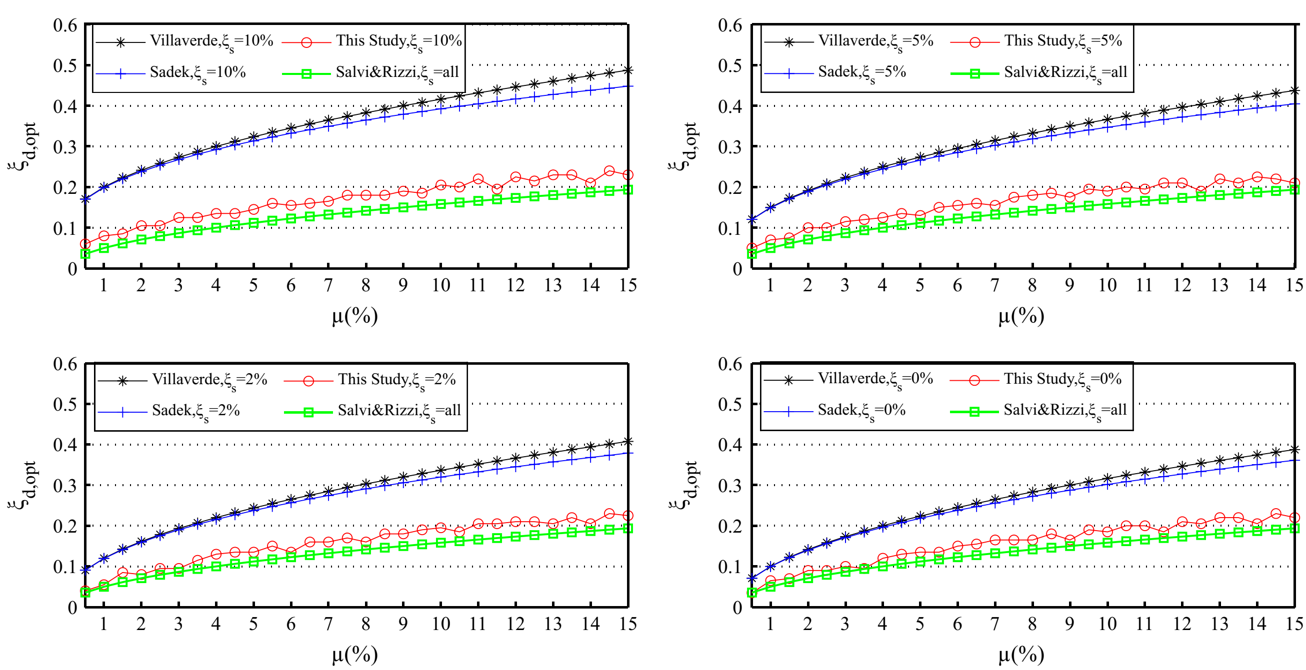

Fig. 5 Optimum damping ratio (ξ_d-opt) as a function of mass ratio (μ) and four at different inherent structural damping ratios

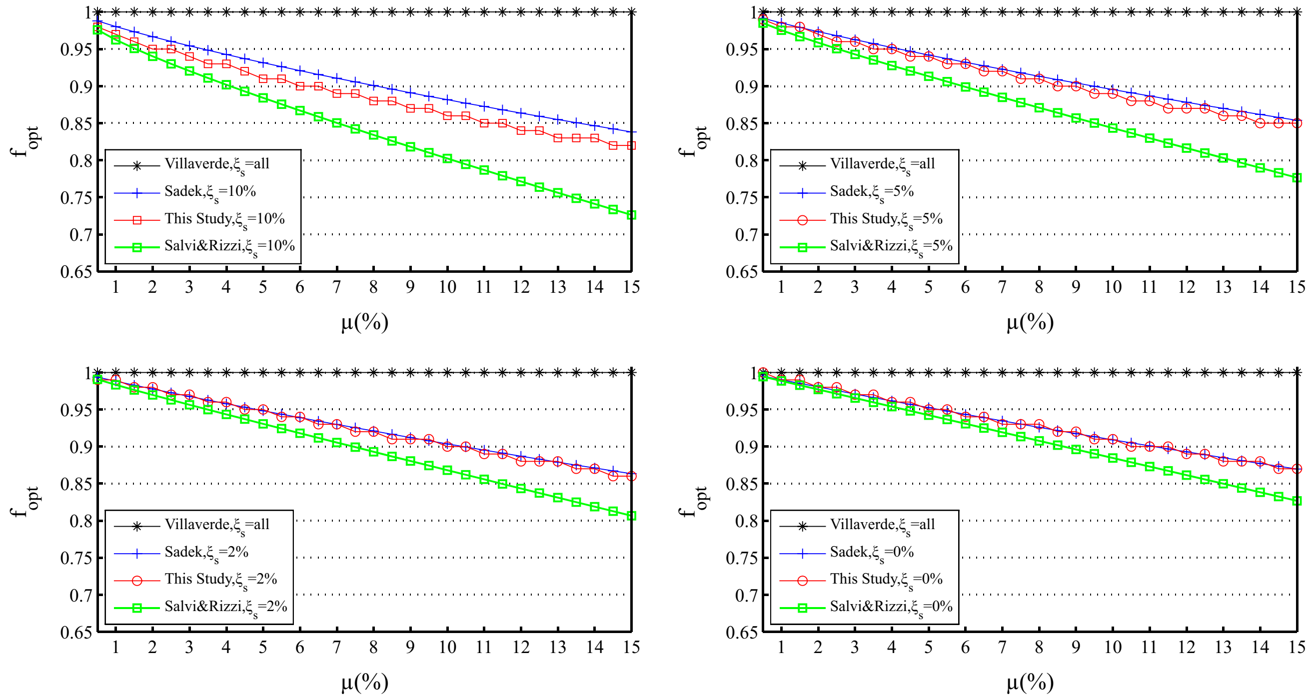

Fig. 6 Optimum frequency ratio (fopt) as a function of mass ratio (μ) and at four different inherent structural damping ratios

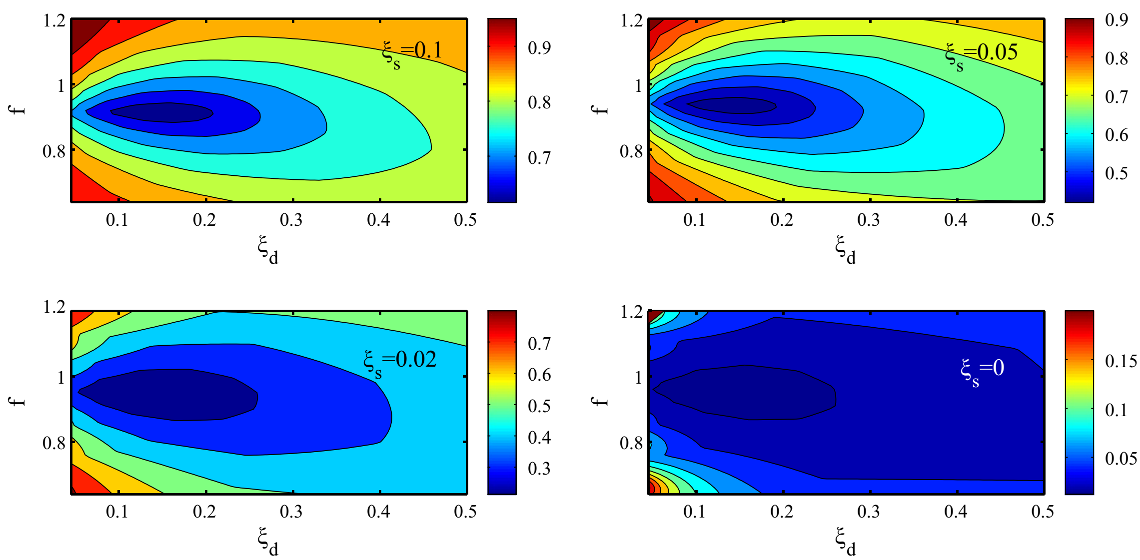

Fig. 7 H_∞ norm ratio of controlled to uncontrolled structure at $\mu = 0.05$ and four different inherent structural damping ratios near the optimum tuning parameter values (ξ_d and f)

approaches may be required to increase the convergence speed, e.g., using initial feasible proper solutions instead of randomly generated initial solutions, using hybrid forms of metaheuristics as an alternative of conventional variants (Kazemzadeh Azad 2017) or considering competitive metaheuristics such as the upper bound strategy (UBS) proposed by Kazemzadeh Azad et al. (2013) or guided stochastic search (GSS) suggested by Kazemzadeh Azad and Hasançebi (2015).

Initial proper feasible solution could be calculated from closed-form formulae presented in Table 1, and seeding these promising starting points could decrease the optimization time considerably. In order to reduce the computational time, the upper bound strategy UBS or GSS can also be

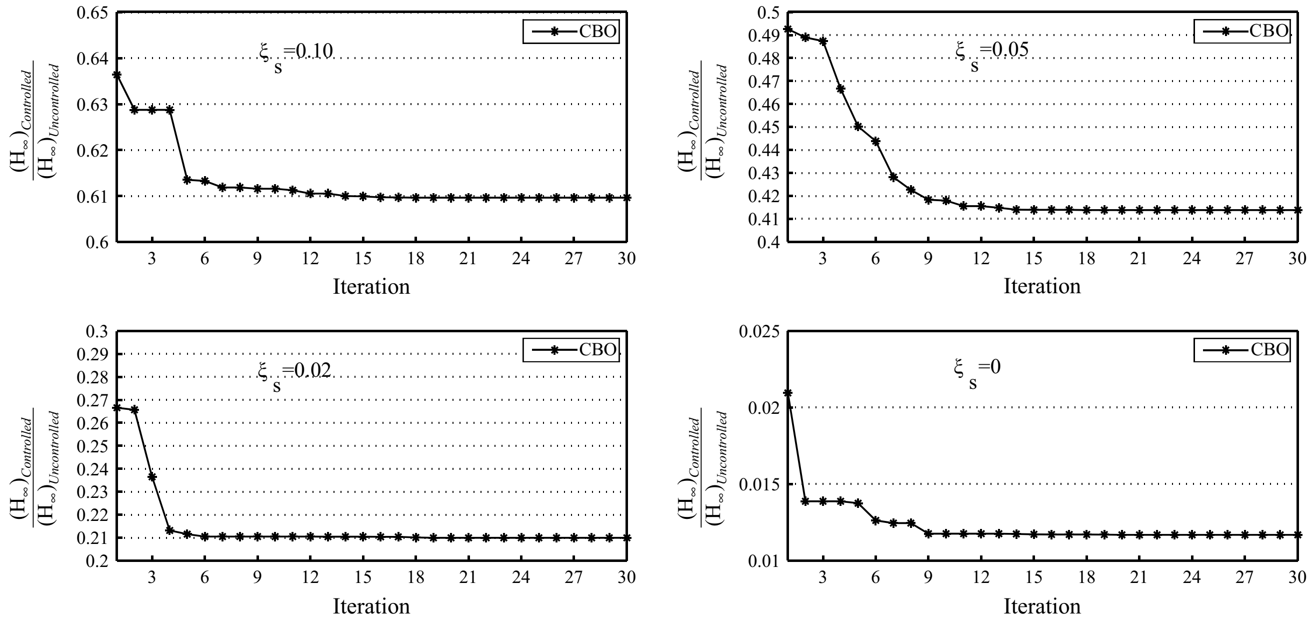

Fig. 8 Convergence history at $\mu=0.05$ and four different inherent structural damping ratios

used. The main issue in the UBS is to detect those candidate designs which have no chance to surpass the best design found so far during the iterations of the optimum design process. After identifying those non-improving designs, they are directly excluded from the structural analysis stage, resulting in a significant savings in the computational effort. UBS is successfully utilized in optimal design of large scale structures (Kaveh and Ilchi Ghaazan 2018).

6 Performance Assessment of Optimum Designed TMD Under Different Earthquakes

In this section, the performance of the controlled 10-story shear building under three far-fault benchmark earthquake excitations (Northridge, Morgan Hill and El Centro) is envisaged based on the attained design graphs from the past section. The peak and root mean square (RMS) building roof displacements are considered as the performance criteria. In Fig. 9, the first 30 s of the selected earthquake records downloaded from peer website are plotted.

In Fig. 10, the roof displacement response history normalized to uncontrolled case is plotted for uncontrolled and controlled structures designed based on different methods and under three different earthquakes at mass and damping ratios equal to 5%.

To make a better comparison between performance and efficiency of different methods, the controlled to uncontrolled maximum roof displacement is calculated and plotted in Figs. 11, 12 and 13 at different mass and damping ratios under the three different earthquakes.

In Fig. 11, four graphs are plotted each of which consider a distinct inherent structural damping ratio, and in each graph, the controlled to uncontrolled maximum roof displacement under Northridge earthquake is calculated by four different methods and with the mass ratios in the range of 0.5–15%. Generally, all methods show a similar trend, and the maximum roof displacement reduces considerably with increasing mass ratio for a specific inherent structural damping ratio. Furthermore, as the inherent structural damping ratio decreases, the effectiveness of the TMD for a particular method increases, i.e., the ordinate decreases for a definite mass ratio within all of the four graphs. Additionally, in all of the graphs, the proposed method of this study has almost the same values as Salvi and Rizzi expressions resulting in the reduction in the maximum response.

Under Morgan Hill and El Centro earthquakes, although the performance of this investigation proposed method is in a good correlation with Salvi and Rizzi's method, this study performed slightly better under the former earthquake; however, both of these methods are dominated by Villaverde and Sadek et al.'s methods. Furthermore, under El Centro excitation the Salvi and Rizzi method has the best performance among all of the compared methods.

To compare the performance of the controlled structure with different methods and under different earthquakes at a specific mass ratio, Fig. 14 is represented. Since the mass ratio is usually considered less than 5% because of construction considerations, these bar charts are plotted for

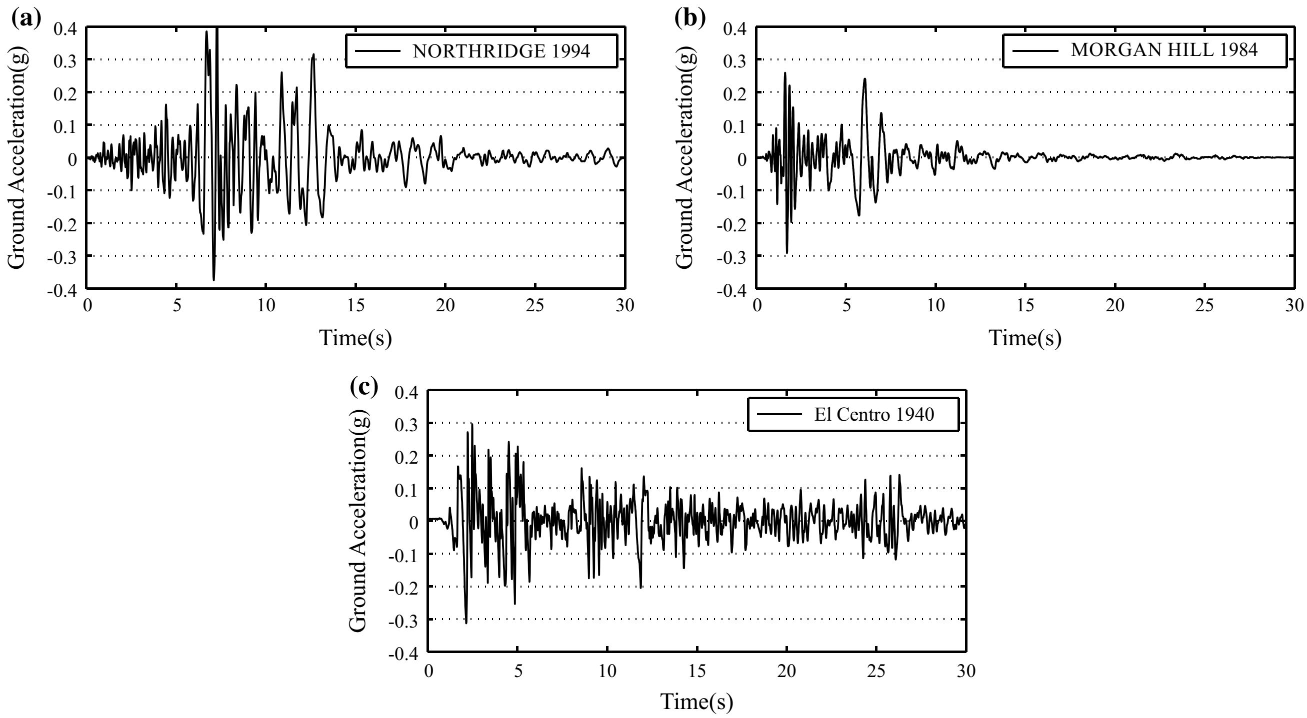

Fig. 9 Accelerogram of three different ground motions: **a** Northridge (1994), **b** Morgan Hill (1984), **c** El Centro (1940)

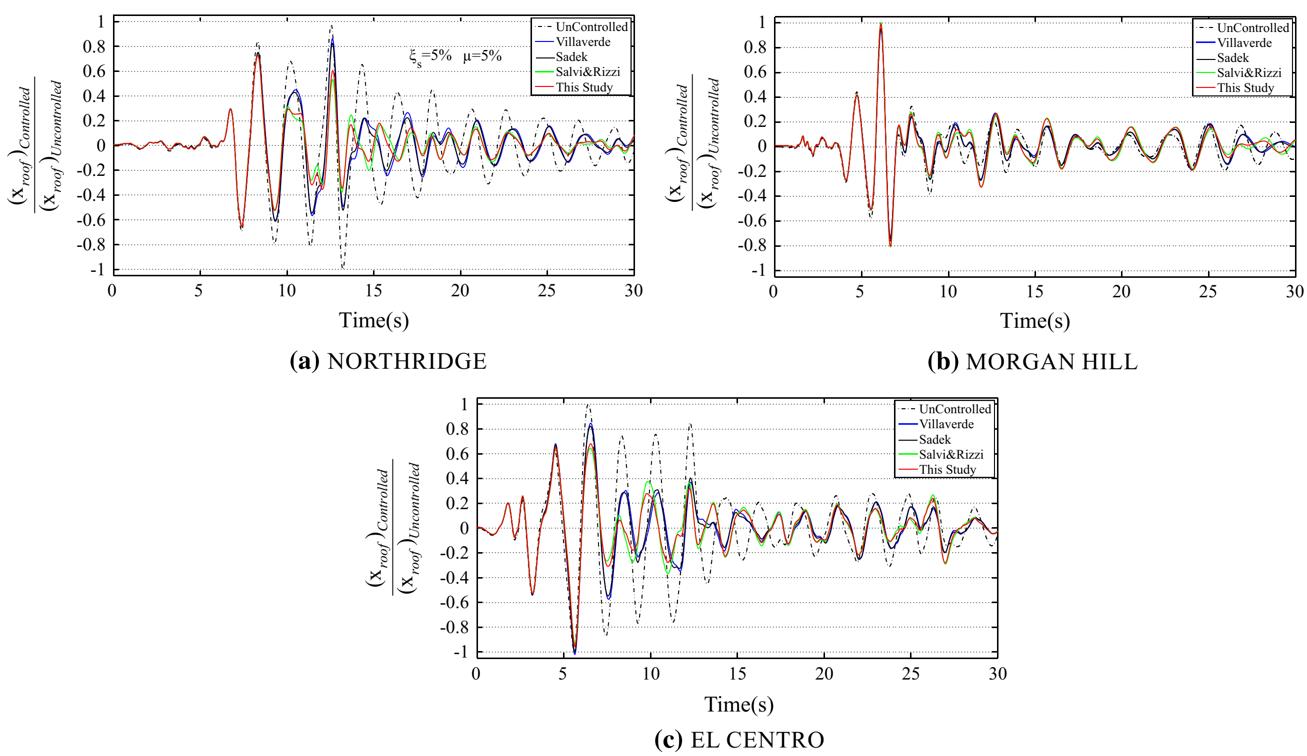

Fig. 10 Normalized roof displacement history of controlled to uncontrolled buildings with different methods under three different earthquakes. Case with $\xi_s = 0.05$ and $\mu = 0.05$

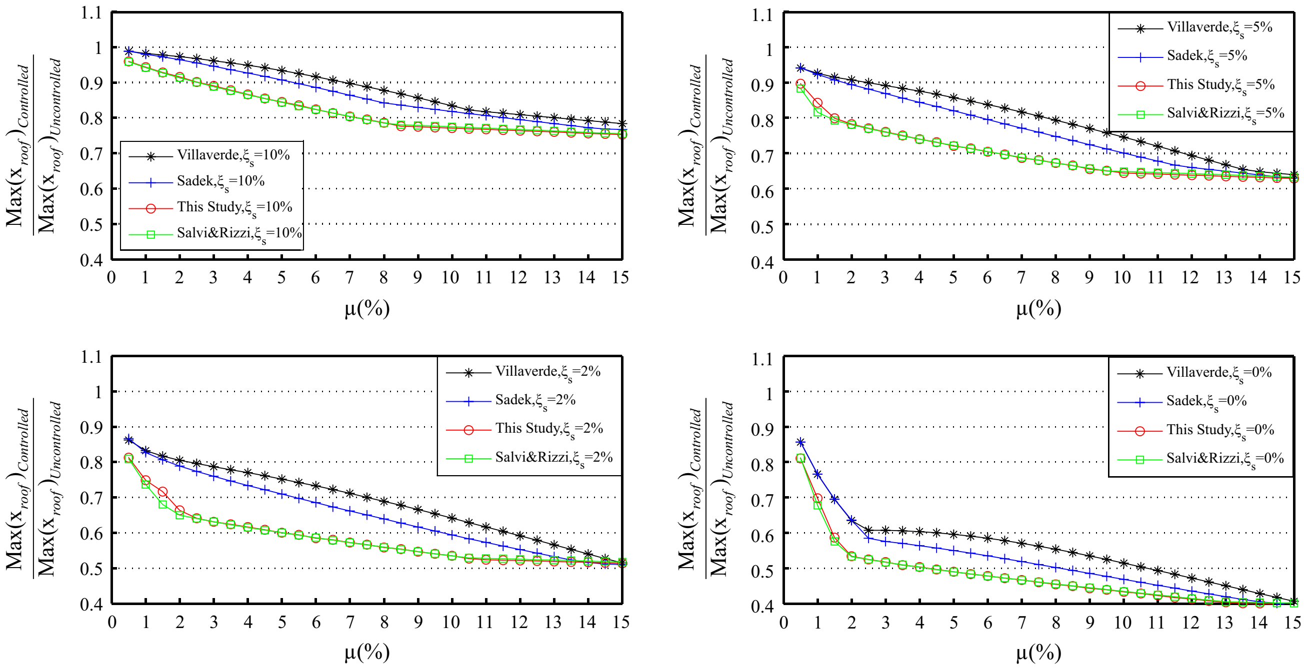

Fig. 11 Normalized maximum roof displacement for different methods as a function of mass ratio (μ) for different inherent structural damping ratios under Northridge (1994)

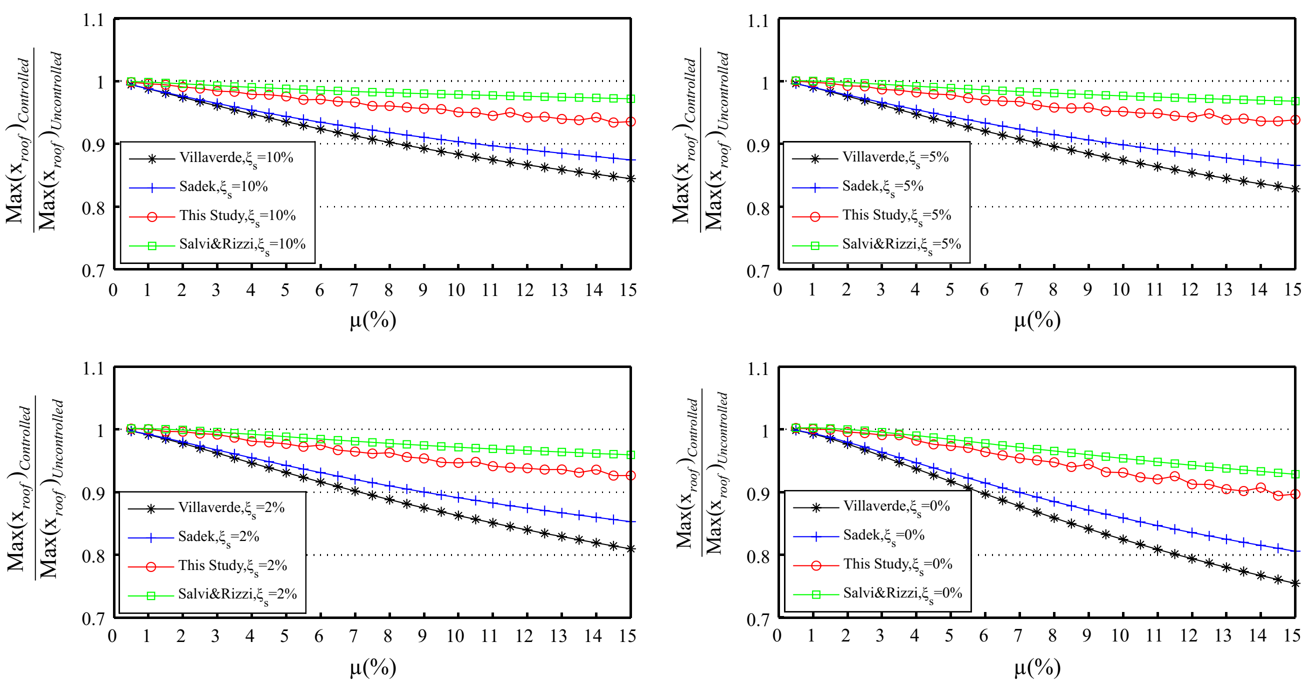

Fig. 12 Normalized maximum roof displacement for different methods as a function of mass ratio (μ) for different inherent structural damping ratios under Morgan Hill (1984)

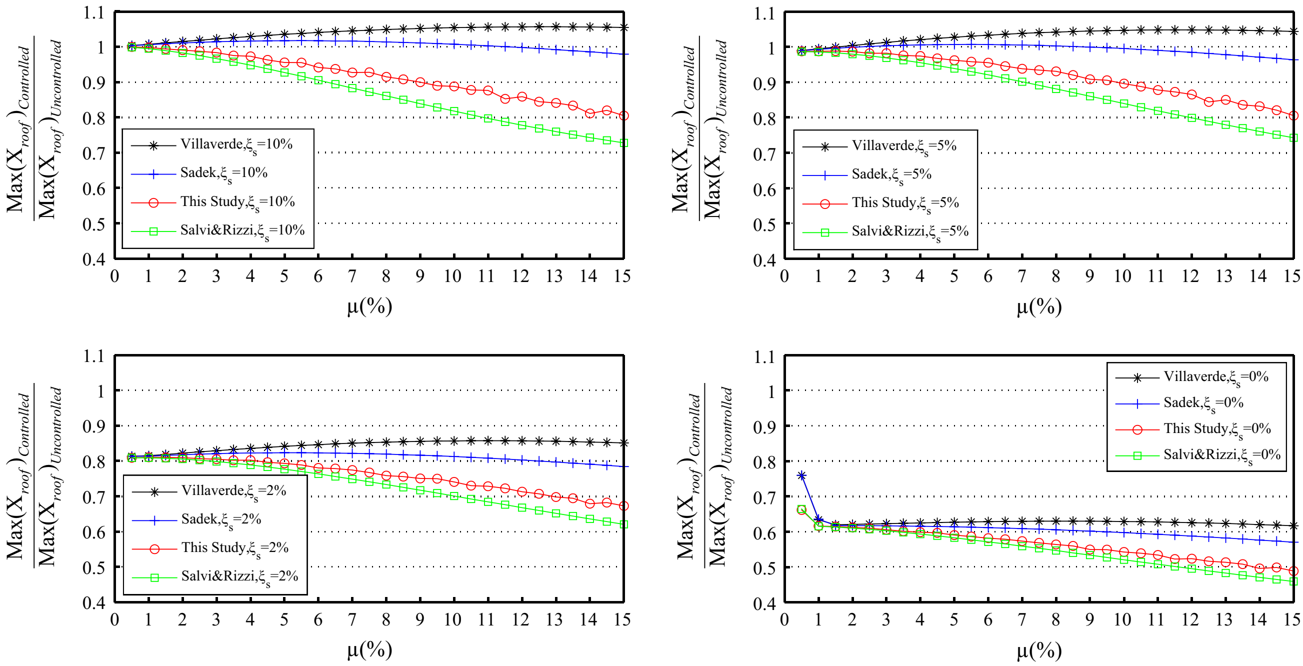

Fig. 13 Normalized maximum roof displacement for different methods as a function of mass ratio (μ) for different inherent structural damping ratios under El Centro (1940)

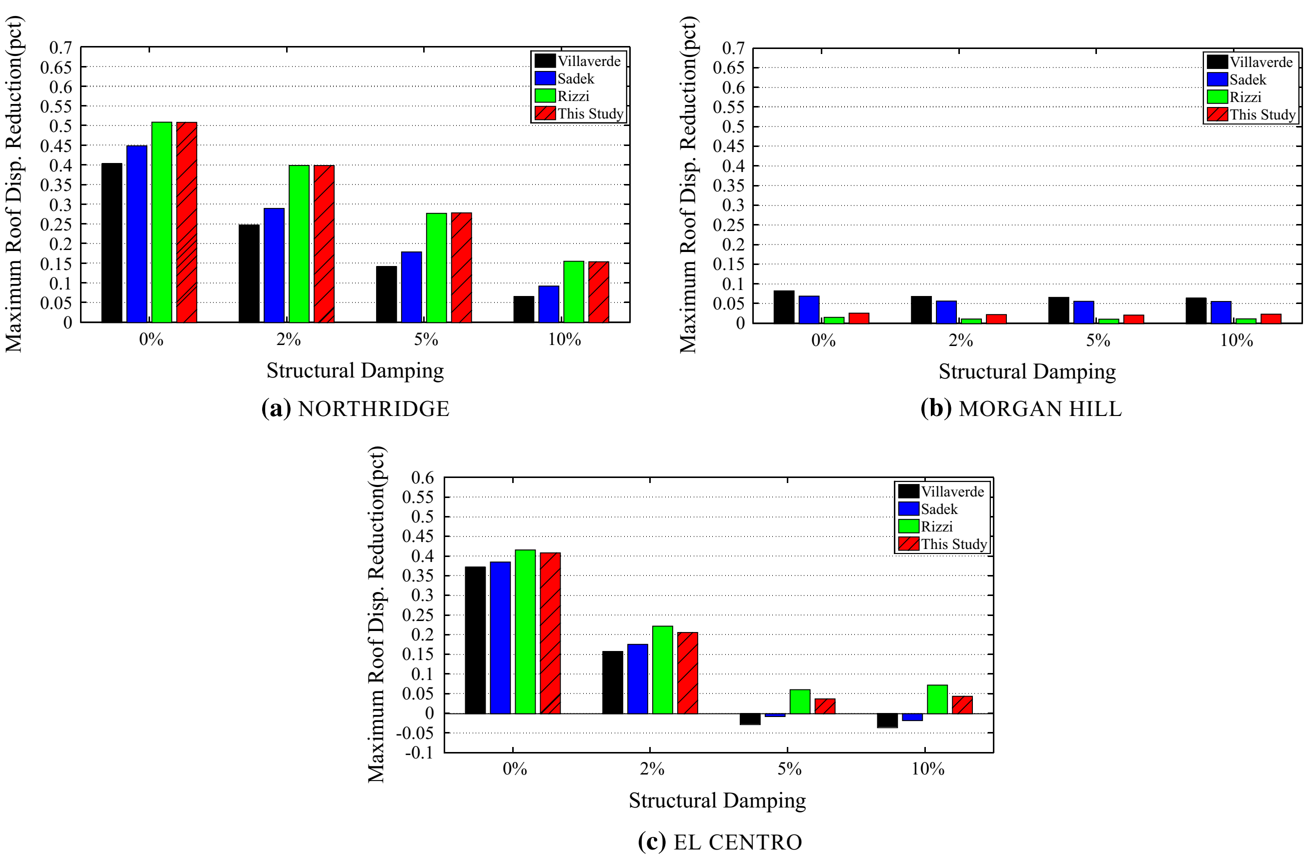

Fig. 14 Maximum roof displacement reduction for different methods, $\mu = 0.05$ and four different inherent structural damping ratios under three different earthquakes: **a** Northridge (1994) **b** Morgan Hill (1984) **c** El Centro (1940)

$\mu = 5\%$. In these charts, horizontal axes represent four different structural damping ratios and vertical axes represent controlled to uncontrolled maximum roof displacement response reduction.

In Fig. 14, for each considered earthquake a bar chart is plotted. It can be seen that under all earthquake excitations, the performance of the TMD is decreased by increasing the inherent structural damping, and even under El Centro excitation, using TMD designed by the Villaverde or Sadek et al. methods increases the displacement response about 1–2% with respect to uncontrolled structure at higher values of inherent structural damping ratios, i.e., these methods have negative performance in response reduction. As stated before, the two methods of Villaverde and Sadek et al. have almost the same performance and their difference is less than 5%. Furthermore, the same statement is true about Salvi and Rizzi and the proposed method in this paper.

Under Northridge excitation, tuning the TMD with the proposed method in this study has the best performance and even for undamped structure, the response is reduced to the half of the uncontrolled structure. However, the efficiency of the TMD is decreased by increasing the inherent structural damping, and finally, in 10% damping, the maximum roof displacement reduction is about 15%.

Under Morgan Hill earthquake, two important points can be observed. Firstly, the efficiency reduction in TMD with increasing inherent structural damping is so smooth, and the amount of response reduction in all damping ratios is so small and is under 10% for all cases. Secondly, in contrast to the two other earthquake excitations, under this earthquake, Villaverde (1985) method has the best performance in comparison with other methods.

Under El Centro excitation, the general pattern is the same as Northridge excitation with the difference being that the Salvi and Rizzi method has the best performance in comparison with other methods. Maximum roof displacement response reduction under this earthquake is for undamped structure, and about 41% reduces the maximum roof displacement. Maximum displacement reduction amount is declined by increasing the inherent structural damping and reaches 7% finally at damping ratio equal to 10%.

Furthermore, in Figs. 15, 16 and 17, the controlled to uncontrolled RMS roof displacement is studied for different mass and inherent structural damping ratios under three different earthquakes and with different methods to assure the good performance of the TMD along the entire record length.

The study of this performance criterion has the same results as the previous criterion, i.e., generally the results of the proposed method in this study are almost similar to the results of the Salvi and Rizzi method. It should be noted that the results of these two methods have the same patterns although in some cases, one is slightly better than the other.

Similar to peak displacement criterion showing the good performance of the proposed method in all considered earthquakes, for RMS criterion, the proposed method has reduced the responses under all the considered earthquakes, though it does not show the best performance under Morgan Hill

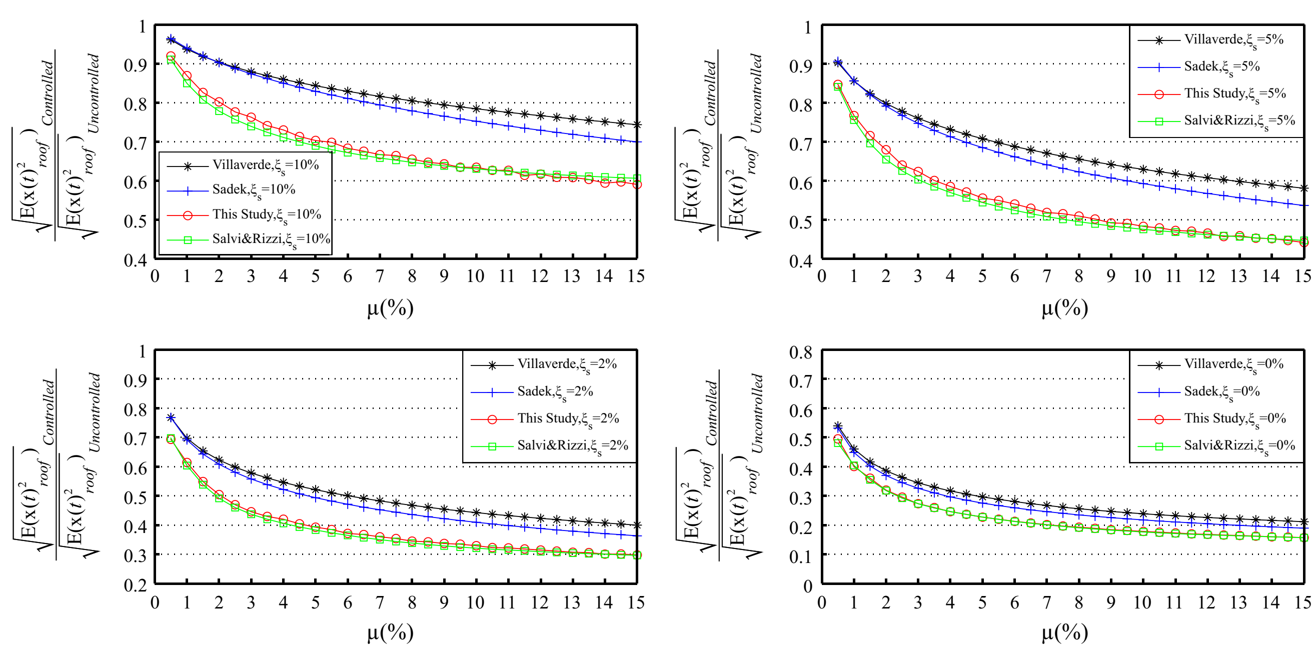

Fig. 15 Normalized controlled to uncontrolled RMS structural roof displacement for different methods as a function of mass ratio (μ) for different inherent structural damping ratios under Northridge (1994)

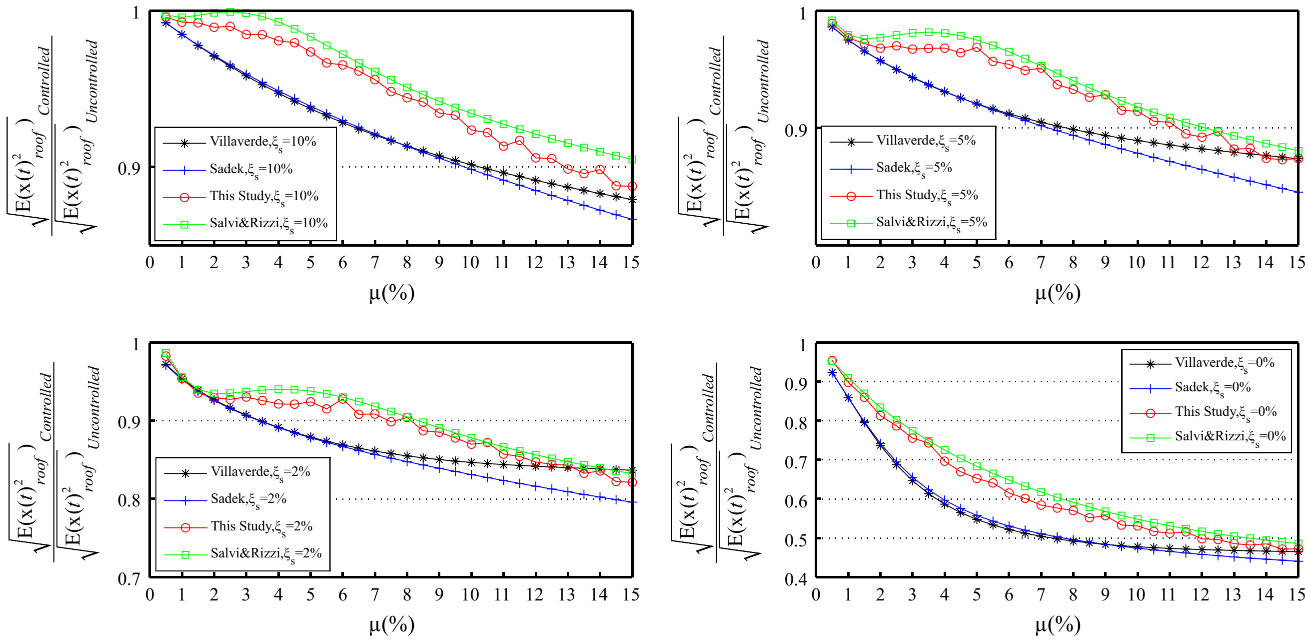

Fig. 16 Normalized controlled to uncontrolled RMS structural roof displacement for different methods as a function of mass ratio (μ) for different inherent structural damping ratios under Morgan Hill (1984)

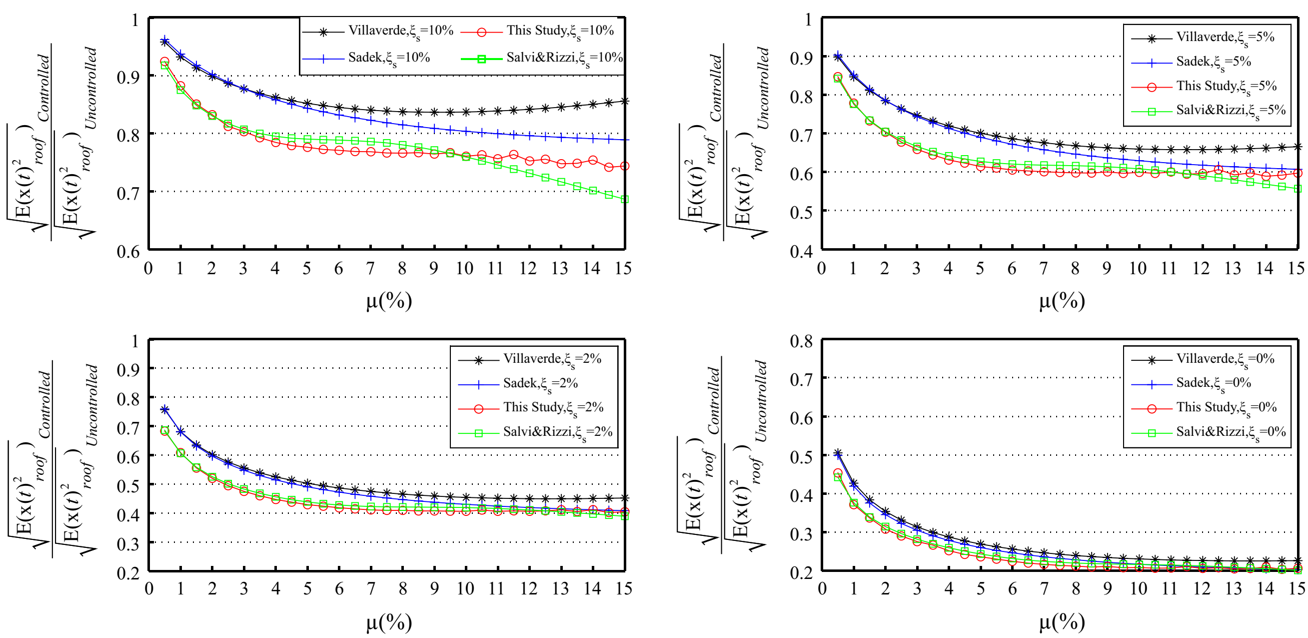

Fig. 17 Normalized controlled to uncontrolled RMS structural roof displacement for different methods as a function of mass ratio (μ) for different inherent structural damping ratios under El Centro (1940)

earthquakes which can be due to the earthquake frequency content and the effect of higher modes in structural response.

Under Morgan Hill earthquake, by considering the RMS criterion, the Villaverde and Sadek et al. methods have better performances in comparison with Salvi and Rizzi and this study approach. However, at mass ratio equal to 15%, the performances of all methods become nearly the same. Additionally, the RMS displacement reduction at controlled structure is much lower in contrast to the other two earthquakes, so generally under this earthquake, TMD has slightly lower performance.

7 Conclusions

This study presents a method for optimum design of a TMD added to the roof of an MDOF structure based on the H_∞ norm minimization of an equivalent SDOF using CBO. Furthermore, with the concept of robust control, this approach reduces the structural response under different earthquake excitations. Two characteristics of this procedure are its simple implementation and fast convergence. In order to assess the performance of the proposed method, two performance criteria (peak and RMS roof displacements) are evaluated for a 10-story shear building subjected to three different earthquake excitations. These criteria are calculated for controlled structure with the proposed framework and other proposed formulae in the literature, and the results are compared in the design charts with each other. The results demonstrate the good performance of the proposed method in most of the considered cases. This method in parallel with Salvi and Rizzi's method finds the TMD optimum parameters in such a way that in most of the cases they dominated the other proposed formula in reducing the structural response. Finally, for the studied building, design charts can be used to obtain the TMD optimum parameters as a function of μ and ξ_s.

Overall, the reported numerical results show the potential of the TMD as a seismic protection system. However, the potentially nonlinear structural response should be accounted for structures under larger earthquake excitations. Furthermore, a detailed seismic performance assessment is required for a 3D model under large set of earthquake ground motions to consider earthquake excitation uncertainty and the uncertainty to the TMD properties. Moreover, investigating the TMD economic performance remains as a topic for the authors' future works utilizing cost-related criteria or other economic benefits of the TMD vis-à-vis the other passive vibration control solutions. These criteria could be considered as optimization objective functions for single and/or multi-objective optimization problems.

References

Arfiadi Y (2016) Reducing response of structures by using optimum composite tuned mass dampers. Procedia Eng 161:67–72

Asami T, Nishihara O, Baz AM (2002) Analytical solutions to H_∞ and H_2 optimization of dynamic vibration absorbers attached to damped linear systems. Struct Control Health Monit 124(3):617–635

Bekdas G, Nigdeli SM (2011) Estimating optimum parameters of tuned mass dampers using harmony search. Eng Struct 33:2716–2723

Bekdas G, Nigdeli SM (2017a) Optimum tuned mass damper design in frequency domain for structures. KSCE J Civ Eng 21(3):912–922

Bekdas G, Nigdeli SM (2017b) Metaheuristic based optimization of tuned mass dampers under earthquake excitation by considering soil-structure interaction. Soil Dyn Earthq Eng 92:443–461

Chopra AK (2001) Dynamics of structures: theory and applications to earthquake engineering, 2nd edn. Prentice Hall, Englewood Cliffs

Debnath N, Deb SK, Dutta A (2013) Frequency band-wise passive control of linear time invariant structural systems with H_∞ optimization. J Sound Vib 332(23):6044–6062

Den Hartog JP (1947) Mechanical vibrations, 3rd edn. McGraw-Hill, New York

Farshidianfar A, Soheili S (2013a) ABC optimization of TMD parameters for tall buildings with soil structure interaction. Int Multiscale Mech 6(4):339–356

Farshidianfar A, Soheili S (2013b) Optimization of TMD parameters for earthquake vibrations of tall buildings including soil structure interaction. Int J Optim Civ Eng 3(3):409–429

Farshidianfar A, Soheili S (2013c) Ant colony optimization of tuned mass dampers for earthquake oscillations of high-rise structures including soil-structure interaction. Soil Dyn Earthq Eng 51(1):14–22

Gutierrez Soto M, Adeli H (2013) Tuned mass dampers. Arch Comput Methods Eng 20(4):419–431

Gutierrez Soto M, Adeli H (2014) Optimum tuning parameters of tuned mass dampers for vibration control of irregular high-rise building structures. J Civ Eng Manag 20(5):609–620

Hadi MNS, Arfiadi Y (1998) Optimum design of absorber for MDOF structures. ASCE J Struct Eng 124:1272–1280

Ioi T, Ikeda K (1978) On the dynamic damped absorber of the vibration system. Bull Jpn Soc Mech Eng 21:64–71

Kaveh A (2017a) Advances in metaheuristic algorithms for optimal design of structures, 2nd edn. Springer, Switzerland

Kaveh A (2017b) Applications of metaheuristic optimization algorithms in civil engineering. Springer, Switzerland

Kaveh A, Ilchi Ghaazan M (2018) Meta-heuristic algorithms for optimal design of real-size structures. Springer, Switzerland

Kaveh A, Mahdavi VR (2014) Colliding bodies optimization method for optimum design of truss structures with continuous variables. Adv Eng Softw 70:1–12

Kaveh A, Mohammadi S, Khadem Hosseini O, Keyhani A, Kalatjari VR (2015) Optimum parameters of tuned mass dampers for seismic application using charged system search. Iran J Sci Technol Trans Civ Eng 39:21–40

Kazemzadeh Azad S (2017) Enhanced hybrid metaheuristic algorithms for optimal sizing of steel truss structures with numerous discrete variables. Struct Multidiscip Optim 55(6):2159–2180

Kazemzadeh Azad S, Hasançebi O (2015) Computationally efficient discrete sizing of steel frames via guided stochastic search heuristic. Comput Struct 156:12–28

Kazemzadeh Azad S, Hasançebi O, Kazemzadeh Azad S (2013) Upper bound strategy for metaheuristic based design optimization of steel frames. Adv Eng Softw 57:19–32

Leung AYT, Zhang H (2009) Particle swarm optimization of tuned mass dampers. Eng Struct 31:715–728

Leung AYT, Zhang H, Cheng CC, Lee YY (2008) Particle swarm optimization of TMD by non-stationary base excitation during earthquake. Earthq Eng Struct Dyn 37:1223–1246

Lu X, Zhang Q, Weng D, Zhou Z, Wang S, Mahin SA, Ding S, Qian F (2016) Improving performance of a super tall building using a new eddy current tuned mass damper. Struct Control Health Monit 24(3):e1940

Nigdeli SM, Bekdas G, Yang XS (2016) Optimum tuning of mass dampers for seismic structures using flower pollination algorithm. Int J Theor Appl Mech 1:264–268

Sadek F, Mohraz B, Taylor AW, Chung RM (1997) A method of estimating the parameters of tuned mass dampers for seismic applications. Earthq Eng Struct Dyn 26(6):617–635

Salvi J, Rizzi E (2011) Minimax optimization of tuned mass dampers under seismic excitation, In: Proceedings of the 8th international conference on structural dynamics, Leuven, Belgium

Salvi J, Rizzi E (2016) Closed-form optimum tuning formulas for passive tuned mass dampers under benchmark excitations. Smart Struct Syst 17(2):231–256

Salvi J, Rizzi E (2017) Optimum earthquake-tuned TMDs: seismic performance and new design concept of balance of split effective modal masses. Soil Dyn Earthq Eng 101:67–80

Soong TT (1990) Active structural control theory and practice, 1st edn. Wiley, New York

Villaverde R (1985) Reduction seismic response with heavily-damped vibration absorbers. Earthq Eng Struct Dyn 13(1):33–42

Warburton GB (1982) Optimum absorber parameters for various combinations of response and excitation parameters. Earthq Eng Struct Dyn 10(3):381–401